

**THEORETICAL CONFIRMATION OF THE REACTION MECHANISM LEADING TO REGIOSELECTIVE FORMATION OF THIAZOLIDIN-4-ONE FROM BROMOACETIC ACID DERIVATIVES**

Ladislav JANOVEC<sup>a1</sup>, Stanislav BÖHM<sup>b</sup>, Ivan DANIHEL<sup>a2</sup>, Ján IMRICH<sup>a3,\*</sup>, Pavol KRISTIAN<sup>a4</sup> and Karel D. KLIKA<sup>c</sup>

<sup>a</sup> Institute of Chemistry, Faculty of Science, P. J. Šafárik University, SK-04167 Košice, Slovak Republic; e-mail: <sup>1</sup> janoveclad@yahoo.com, <sup>2</sup> ivan.danihel@upjs.sk, <sup>3</sup> jan.imrich@upjs.sk, <sup>4</sup> pavol.kristian@upjs.sk

<sup>b</sup> Department of Organic Chemistry, Institute of Chemical Technology, Prague, CZ-16628 Prague 6, Czech Republic; e-mail: bohm@vscht.cz

<sup>c</sup> Department of Chemistry, University of Turku, FIN-20014 Turku, Finland; e-mail: karel.klika@utu.fi

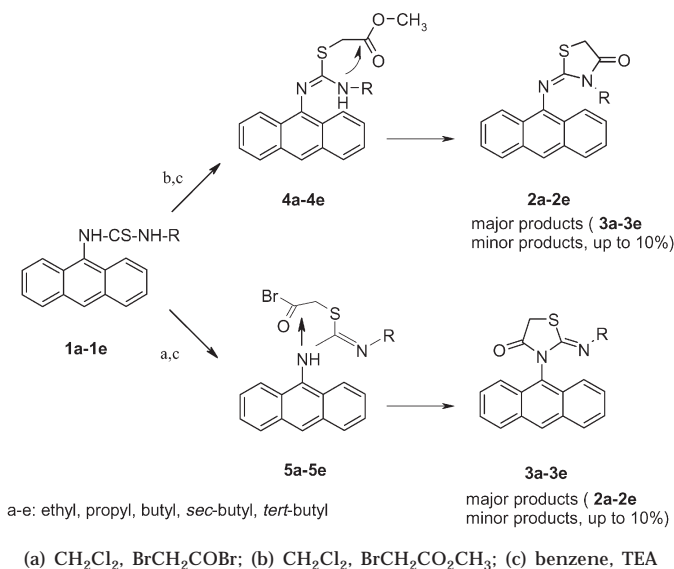
Received May 15, 2007  
Accepted October 8, 2007

A regioselective synthesis of 3-alkyl-2-[(anthracen-9-yl)imino]thiazolidin-4-ones **2a–2e** and 2-(alkylimino)-3-(anthracen-9-yl)thiazolidin-4-ones **3a–3e** from appropriate thioureas using methyl bromoacetate or bromoacetyl bromide, respectively, has been rationalized by DFT calculations of model thiourea and its phenyl derivative. The proposed mechanism indicates that the regioselective formation of the target thiazolidinones is a consequence of a different reactivity of the reagents and a varying stability of the intermediates, 1-alkyl-3-(anthracen-9-yl)-2-[(methoxycarbonyl)methyl]isothiureas **4a–4e** and 1-alkyl-3-(anthracen-9-yl)-2-(bromoacetyl)isothiureas **6a–6e**.

**Keywords:** B3LYP functional; Bromoacetic acid; DFT calculations; Reaction mechanisms; Regioselectivity; Thiourea; Thiazolidinone.

As a part of our ongoing project regarding the synthesis of novel intercalating thiazolidinones, the results of the treatment of thiourea **1** with bromoacetic acid derivatives were reported (Scheme 1)<sup>1,2</sup>. The essence of that study was that the regioselective formation of **2a** or **3a** depended on the used reagent. Whilst the treatment of **1a** with methyl bromoacetate provided mostly 2-[(anthracen-9-yl)imino]-3-ethylthiazolidin-4-one (**2a**), the reaction with bromoacetyl bromide contrastingly afforded major 3-(anthracen-9-yl)-2-(ethylimino)thiazolidin-4-one (**3a**) as confirmed by X-ray analysis<sup>1</sup>. The high regioselectivity was underscored by the fact that in both reactions only up to 10% of the other regioisomer was formed. A controlled regioselective synthesis of biologically active 2,3-disubstituted

2-iminothiazolidin-4-ones is still rather unattainable despite many papers devoted to this problem. Our results, giving rise to the possibility of new synthetic strategy for the predictable preparation of regioisomeric thiazolidin-4-ones, prompted us to explore in detail the regioselectivity based on both experimental observations and computational chemical methods.



SCHEME 1

An explanation of the regioselectivity has intuitively resulted from the rules of the Pearson HSAB theory<sup>3,4</sup>. As depicted in Scheme 1, the initial assumption proposes the formation of isothioureas **4a-4e** and **5a-5e** as a consequence of the anticipated initial soft attack by sulfur with subsequent cyclization owing to a hard interaction between the nitrogen nucleophile and electrophilic carbonyl carbon. Notwithstanding, this concept offers a reasonable explanation of the experimental observations but, nonetheless, is worth further detailed investigation. In continuation therefore, we present here an assessment of the mechanistic hypotheses proposed to explain the previous experimental results<sup>1</sup>, which is based on the density functional theory (DFT) calculations.

## RESULTS AND DISCUSSION

The observation of different products and, hence, probably different reaction pathways focused our attention to the reactivity of bromoacetic acid

derivatives. To gain insight into the regioselective formation of thiazolidin-4-ones **2a** and **3a**, we monitored the structural changes of thiourea **1a** substrate during the course of its reaction with both methyl bromoacetate and bromoacetyl bromide leading to the formation of **2a** and **3a**. Monitoring was accomplished by  $^1\text{H}$  NMR spectroscopy in  $\text{CDCl}_3$  at room temperature and the evaluation of the process was based on the changes in the intensities of the methylene signals of thiourea **1a**, isothioureas **4a** and **5a**, and thiazolidin-4-ones **2a** and **3a**. Although in Experimental one-pot preparation of thiazolidin-4-ones is described, we performed monitoring as a two-step process to simplify  $^1\text{H}$  NMR spectra with separate addition of triethylamine enabling the second cyclization step.

In the reaction with methyl bromoacetate, the insight was also obtained by observation of the NH proton signals. As the reaction progressed, the NH proton signals disappeared as a consequence of the formation of isothiuronium salt. However, after addition of triethylamine, the NH proton signal of free isothiourea **4a** re-emerged near to its previous chemical shift, but it again disappeared as the cyclization reaction progressed. The preferred location of the NH hydrogen in free isothiourea **4a** on the nitrogen bearing ethyl rather than on the nitrogen bearing anthracenyl might be, in addition to resonance stabilization of the double bond with the aromatic anthracenyl moiety, due to a  $\pi$ -NH intramolecular hydrogen bond. The presence of such intramolecular hydrogen bond would certainly account for the direct observation of the NH proton under conditions when its likely rate of exchange would be expected to render it unobservable as a distinct signal (i.e. after addition of triethylamine). As a consequence of these observations, it is evident that the nitrogen atom bearing ethyl is  $\text{sp}^3$ -hybridized and that the nitrogen bearing anthracenyl is  $\text{sp}^2$ -hybridized, as portrayed in Fig. 1.

As depicted in Fig. 2, the treatment of thiourea **1a** with an equimolar amount of methyl bromoacetate was relatively slow with the reaction half-time of ca. 300 min, reaching completion in ca. 3000 min. The formation of thiazolidin-4-one **2a** proceeded at a considerably higher rate after removal of hydrobromide from isothiourea **4a** with triethylamine, with a reaction half-time of ca. 40 min and completion in ca. 200 min. By contrast, the reaction of thiourea **1a** with bromoacetyl bromide under the same conditions was too fast to be monitored by  $^1\text{H}$  NMR. Such observation suggests that, in comparison to methyl bromoacetate, the rate of the reaction with bromoacetyl bromide, higher by orders of magnitude, is not result of alkylation, but, rather of acylation.

To verify this assertion, we examined the reaction pathways using computational chemistry. As the model for our study, unsubstituted thiourea was selected to enable the use of the highly accurate, but expensive, triple zeta 6-311++(2d,2p) basis set exploiting DFT. Both alkylation and acylation for both bromoacetic acid derivatives were considered. The results are summarized in Table I and Figs 3 and 4. We have considered the most simple approximation of acylation as a one-step process to obtain initial point for the next precise elucidation including addition-elimination mechanism and solvation model. For the same reason we have used thiourea as a thione although the most preferred form in the reaction was probably a thiol form. For acylation, the transition state was found to adopt a six-membered structure incorporating a thione thiourea form (Fig. 4). From these results it can be deduced that *S*-alkylation ( $\Delta\Delta G^\ddagger = 44.2 \text{ kJ mol}^{-1}$ ) is

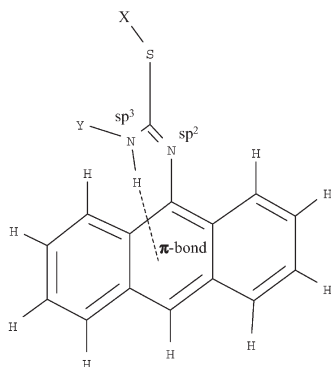


FIG. 1

View of the proposed intramolecular  $\pi$ -NH interaction with subsequent differential hybridization of the nitrogens (X, reagent; Y, alkyl substituent)

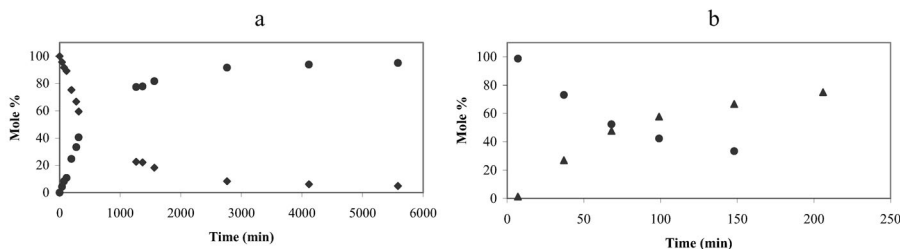


FIG. 2

The formation of isothiurea (a) and thiazolidinone (b) in the reaction of thiourea **1a** with methyl bromoacetate. The concentrations of thiourea **1a** (♦), isothiurea **4a** (●), and thiazolidin-4-one **2a** (▲) versus time were determined by  $^1\text{H}$  NMR

the main pathway for the reaction of thiourea with methyl bromoacetate (Table I, Fig. 3).

The reaction of bromoacetyl bromide was studied similarly as in the previous case. As follows from the computational results, the reactivity of bromoacetyl bromide affords the acylation product ( $\Delta\Delta G^\ddagger = 56.9$  kJ mol<sup>-1</sup>). The interesting point to note is that the alkylation activation energies are relatively close ( $\Delta\Delta G^\ddagger = 3.7$  kJ mol<sup>-1</sup>), reflecting only a minor influence of different substituents on the carbonyl carbon. On the other hand, the large

TABLE I  
Relative Gibbs free energies (kJ mol<sup>-1</sup>) of stationary points on the reaction coordinate of the thiourea reaction with bromoacetyl bromide (bab) or methyl bromoacetate (mba) obtained by B3LYP/6-311++G(2d,2p)

Reactant <sup>a</sup>	$\Delta G_{\text{alkylation}}$	$\Delta G^\ddagger_{\text{alkylation}}$	$\Delta G_{\text{acylation}}$	$\Delta G^\ddagger_{\text{acylation}}$	$\Delta\Delta G$	$\Delta\Delta G^\ddagger$
bab	37.1	140.4	46.5	83.5	9.4	56.9
mba	42.8	144.1	97.9	188.3	55.1	44.2

<sup>a</sup> Energy of reactants 0 kJ mol<sup>-1</sup>.

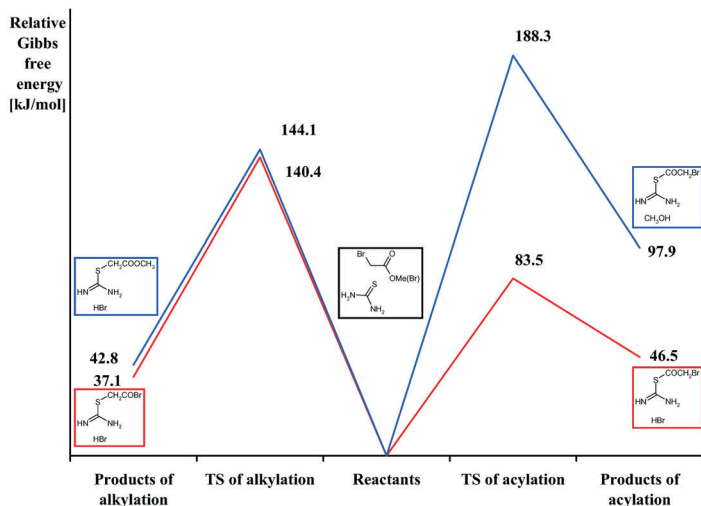


FIG. 3  
Relative Gibbs free energies (B3LYP/6-311++G(2d,2p)) of the stationary points on the reaction coordinate (for better comparison the energies of reactants are defined as equal) of the thiourea reaction with bromoacetyl bromide (red line) and methyl bromoacetate (blue line)

energy gap ( $\Delta\Delta G^\ddagger = 104.8 \text{ kJ mol}^{-1}$ ) of the acylation reaction barriers reflects a large dependence on the electronic effects of the attached substituents (see also data for  $\Delta G^\ddagger_{\text{alkylation}}$  and  $\Delta G^\ddagger_{\text{acylation}}$ ).

Taking into account all the above, the following conclusion is drawn. The formation of thiazolidinones **2a–2e** proceeds by intramolecular cyclization via the  $sp^3$ -hybridized nitrogen of the unstable *S*-alkylisothio-urea obtained by the attack of the sulfur atom on the methylene carbon of methyl bromoacetate (Scheme 1). On the other hand, the reactions of bromoacetyl bromide with thioureas **1a–1e** progress as acylations via carbonyl carbon, in good agreement with  $^1\text{H}$  NMR experiments and the computational results. The next step in this reaction might be anticipated to be cyclization, in analogy to the methyl bromoacetate reaction, which leads to products **8a–8e**. However, these products have never been detected, thus

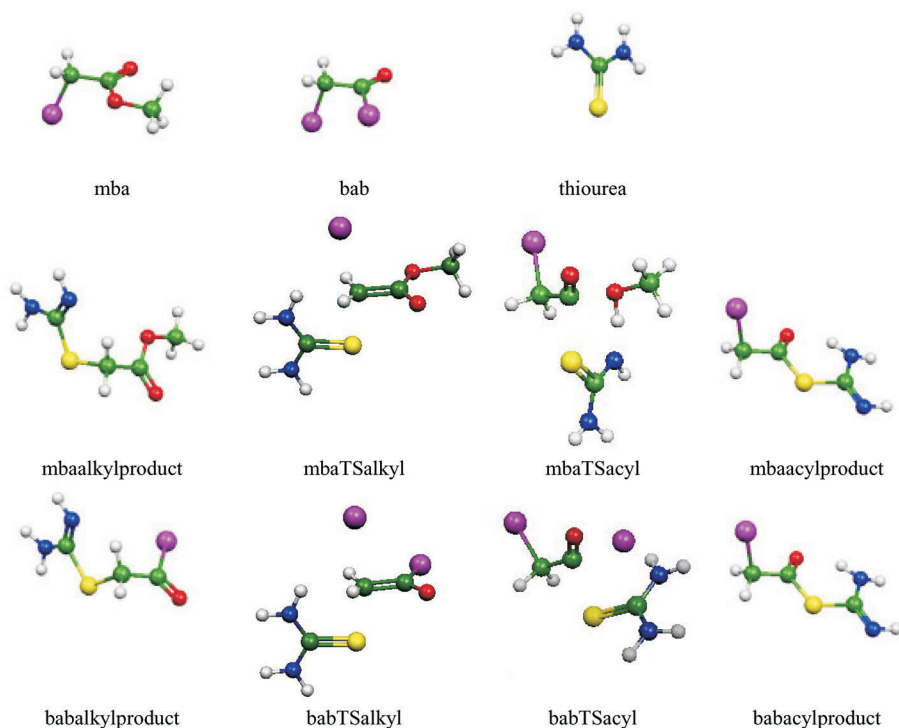
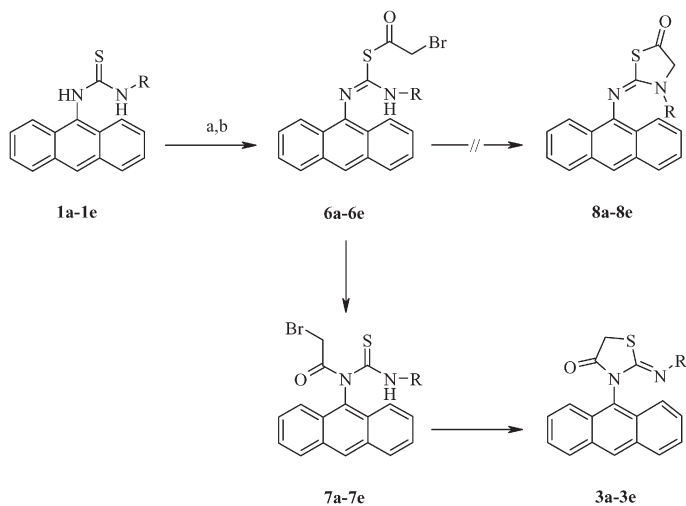


FIG. 4

Geometries of the transition states in the thiourea reaction with bromoacetyl bromide and methyl bromoacetate as obtained by DFT calculations using the B3LYP/6-311G++(2d,2p) basis set

implying the presence of a further reaction step to account correctly for the regioselective formation of compounds **3a–3e** (Scheme 2). The additional step which fulfils the requirement of regioselectivity is an S→N rearrangement<sup>1</sup>, which preferentially occurs on an sp<sup>2</sup>-hybridized nitrogen<sup>5,6</sup> (Scheme 2).



(a) CH<sub>2</sub>Cl<sub>2</sub>, BrCH<sub>2</sub>COBr; (b) benzene, TEA

SCHEME 2

In accordance with our proposed mechanism, the underlying premise directing the regioselectivity of the bromoacetyl bromide reaction is the rearrangement itself. We assumed the rearrangement proceeded onto an isothiurea imino nitrogen correspondingly to other authors<sup>5,6</sup>. To evaluate the migration of the bromoacetyl moiety to this sp<sup>2</sup>-hybridized nitrogen, only theoretical description by DFT calculations (B3LYP/6-31G(d,p)) could be utilized because immediate intramolecular cyclization occurring after rearrangement precluded experimental observation by <sup>1</sup>H NMR. To save the computational time we chose to replace in calculations the anthracenyl moiety with a phenyl. So we obtained the model compound, *S*-(bromoacetyl)-1-phenyl-3-propylisothiurea. The following criteria for geometry optimization of the calculated structures were used:

- an *E* configuration of the C=N double bond between the substituent at the sp<sup>2</sup>-hybridized nitrogen and the sulfur atom, as only in this case the rearrangement is possible;

- an *s-cis* conformation between the carbonyl carbon and the  $sp^2$ -hybridized nitrogen atom;
- the placement of the substituents, to limit steric hindrance, at the  $sp^2$ - and  $sp^3$ -hybridized nitrogen atoms on the opposite the sides of the plane formed by the  $Nsp^2$ -C- $Nsp^3$  atoms.

The results shown in Table II indicate that the regioselectivity of the **3a–3e** formation is neither a consequence of the thermodynamic ( $\Delta\Delta G = -1.2$  kJ mol<sup>-1</sup>) nor kinetic ( $\Delta\Delta G^\ddagger = 2.2$  kJ mol<sup>-1</sup>) advantage of the R1-P1

TABLE II

Relative Gibbs free energies (kJ mol<sup>-1</sup>) of stationary points on the reaction coordinate of the bromoacetyl migration of *S*-(bromoacetyl)-1-phenyl-3-propylisothiurea in *s-cis* phenylimino (Ph) and *s-trans* propylimino form (Pr) obtained by B3LYP/6-31G(d,p) method for combined (I) and separated (II) reaction comparisons

Comparison I	$\Delta G_{\text{reactant}}$	$\Delta G^\ddagger$	$\Delta G_{\text{product}}$	Comparison II	$\Delta G_{\text{reactant}}$	$\Delta G^\ddagger$	$\Delta G_{\text{product}}$
Ph	0	40.9	-52.9	Ph	0	40.9	-52.9
Pr	18.7	61.8	-35.4	Pr	0	43.1	-54.1

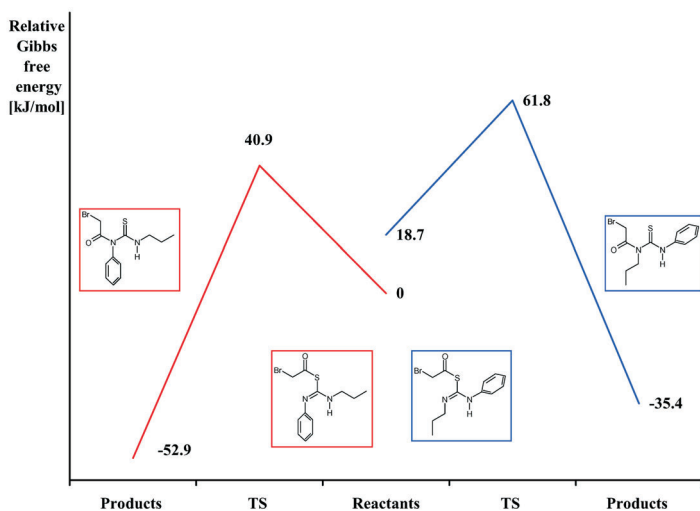


FIG. 5

Relative Gibbs free energies (B3LYP/6-311++G(2d,2p)) of the stationary points on the reaction coordinate of the *S*-(bromoacetyl)-1-phenyl-3-propylisothiurea rearrangement in *s-cis* phenylimino (C-S, red line) and *s-trans* propylimino (C-S, blue line) conformation



route in comparison with the R2–P2 path. The DFT calculations indicate that the regioselectivity is a consequence of the isothiourea propensity to preferably adopt the R1 conformation stabilized ( $\Delta G(\text{R2-R1}) = 18.7 \text{ kJ mol}^{-1}$ ) by resonance of the C=N double bond with the anthracenyl moiety and the  $\pi$ -HN intramolecular bond mentioned before (Figs 5 and 6, Table II).

In consideration of the influence of steric hindrance on the regioselectivity, it was ascertained on the basis of  $^1\text{H}$  NMR measurements of the crude reaction mixtures of compounds **3a–3e**, that the bulkiness of the alkyl substituents has no significant effect on the ratio of the regioisomers. The transition state structures readily provide an explanation for this observation (Fig. 6) as the substituents are located away from and out of the range of the reaction site. Similar behavior was also observed for the reactions with methyl bromoacetate.

In conclusion, the reaction model based on experimental data and computational studies properly describes the observed regioisomerization of thiazolidinones **2a–2e** and **3a–3e**. Very simple model used here as a first approximation, rationalizes our own experimental results and can thus be used as a suitable tool for the design of new synthetic routes in the preparation of analogous heterocyclic compounds.

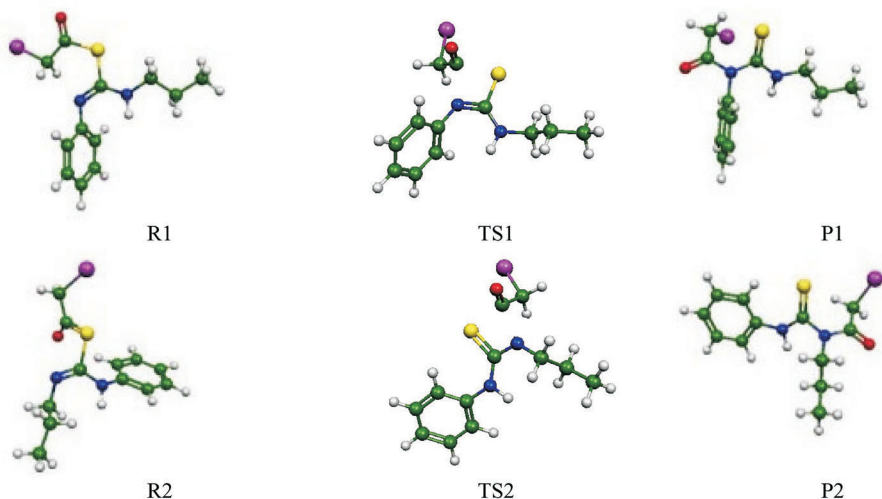


FIG. 6

Geometries of the reactants, products, and transition states of the bromoacetyl migration of the *S*-(bromoacetyl)-1-phenyl-3-propylisothiourea obtained by B3LYP/6-31G(d,p) optimization

## EXPERIMENTAL

Melting points were determined with a Boetius hot-stage apparatus and are uncorrected.  $^1\text{H}$  (300 MHz) and  $^{13}\text{C}$  (75 MHz) NMR spectra were measured using a Varian Gemini 2000 NMR spectrometer, at room temperature in  $\text{CDCl}_3$  using TMS as an internal standard (0 ppm for both nuclei). Elemental analysis was done on a Perkin-Elmer analyzer CHN 2400. The reactions were monitored by thin-layer chromatography (TLC) using Silufol plates with detection at 254 nm. Preparative column chromatography was performed using silica gel Merck (pore volume 60 Å, particle size 63–200  $\mu\text{m}$ ). IR spectra were measured using a Specord 75 IR spectrophotometer (Zeiss) in  $\text{CDCl}_3$ . Bromoacetyl bromide and methyl bromoacetate were commercial products (Aldrich) whilst the starting thioureas **1a–1e** were prepared according to literature<sup>7</sup>. For computational studies, the Gaussian program was used<sup>8</sup> with DFT based on Becke's three-parameter exchange correlation functional B3LYP<sup>9</sup>. The transition states were confirmed by vibrational analysis of the optimized geometries whereby only one negative vibration was obtained in each case. The thermochemistry was computed at 298.15 K with a scale factor of 1.

Improved Method for the Preparation of 3-Alkyl-2-[(anthracen-9-yl)imino]-thiazolidin-4-ones **2a–2e**

Methyl bromoacetate (0.41 mmol) was added to a stirred solution of thiourea **1a–1e** (0.34 mmol) and triethylamine (0.34 mmol) in dichloromethane (5 ml). After the reaction was complete as determined by TLC (eluent benzene–acetone 5:2), the precipitate formed was filtered off, washed with diethyl ether and purified by column chromatography on silica gel using benzene as mobile phase. The reaction was carried out as a one-pot reaction and was more simple and time-saving in comparison with a previous two-step one<sup>1</sup>. All physicochemical characteristics of compounds **3a–3e** were in accordance with the published results<sup>1</sup>.

Improved Method for the Preparation of 3-(Anthracen-9-yl)-2-(alkylimino)-thiazolidin-4-ones **3a–3e**

To a solution of bromoacetyl bromide (0.41 mmol) in dry chloroform (5 ml), triethylamine (0.68 mmol) was added dropwise at  $-10\text{ }^\circ\text{C}$ , followed by the addition of thiourea **1a–1e** (0.34 mmol). After 40 min, triethylammonium bromide formed was removed by flash chromatography on silica gel using benzene as mobile phase. The solvent was removed from appropriate fractions by evaporation in vacuo and the product was purified by recrystallization from a dichloromethane–*n*-heptane (ca. 3:1 v/v) mixture. Similarly to previous, such one-pot procedure simplified obtaining of products with a comparable regioselectivity.

*The present work was supported by the Grant Agency of the Ministry of Education, Slovak Republic (grant No. 1/2471/05) and the State Programme NMR No. 2003SP200280203/2.*

## REFERENCES

1. Klika K. D., Janovec L., Imrich J., Suchár G., Kristian P., Sillanpää R., Pihlaja K.: *Eur. J. Org. Chem.* **2002**, 1248.

2. Klika K. D., Valtamo P., Janovec L., Suchár G., Kristian P., Imrich J., Kivelä H., Alföldi J., Pihlaja K.: *Rapid Commun. Mass Spectrom.* **2004**, *18*, 87.
3. Pearson R. G.: *J. Am. Chem. Soc.* **1963**, *85*, 3533.
4. Pearson R. G., Songstad J.: *J. Am. Chem. Soc.* **1967**, *89*, 1827.
5. Pratt R. F., Bruice T. C.: *J. Am. Chem. Soc.* **1972**, *94*, 2823.
6. Kaválek J., Jirman J., Štěřba V.: *Collect. Czech. Chem. Commun.* **1985**, *50*, 766.
7. Janovec L., Suchár G., Imrich J., Kristian P., Sasinková V., Alföldi J., Sedlák E.: *Collect. Czech. Chem. Commun.* **2002**, *67*, 665.
8. Frisch M. J., Trucks G. W., Schlegel H. B., Scuseria G. E., Robb M. A., Cheeseman J. R., Zakrzewski V. G., Montgomery J. A., Jr., Stratmann R. E., Burant J. C., Dapprich S., Millam J. M., Daniels A. D., Kudin K. N., Strain M. C., Farkas O., Tomasi J., Barone V., Cossi M., Cammi R., Mennucci B., Pomelli C., Adamo C., Clifford S., Ochterski J., Petersson G. A., Ayala P. Y., Cui Q., Morokuma K., Malick D. K., Rabuck A. D., Raghavachari K., Foresman J. B., Cioslowski J., Ortiz J. V., Baboul A. G., Stefanov B. B., Liu G., Liashenko A., Piskorz P., Komaromi I., Gomperts R., Martin R. L., Fox D. J., Keith T., Al-Laham M. A., Peng C. Y., Nanayakkara A., Gonzalez C., Challacombe M., Gill P. M. W., Johnson B., Chen W., Wong M. W., Andres J. L., Gonzalez C., Head-Gordon M., Replogle E. S., Pople J. A.: *Gaussian 98*, Revision A.7. Gaussian, Inc., Pittsburgh (PA) 1998.
9. Becke A. D.: *J. Chem. Phys.* **1993**, *98*, 5648.